Adaptive Color Space Transform using Independent Component Analysis

Esteban Vera Sergio Torres

Department of Electrical Engineering
University of Concepcion, Chile

ABSTRACT

In this paper, a novel color space transform is presented. It is an adaptive transform based on the application of independent component analysis to the *RGB* data of an entire color image. The result is a linear and reversible color space transform that provides three new coordinate axes where the projected data is as much as statistically independent as possible, and therefore highly uncorrelated. Compared to many non-linear color space transforms such as the *HSV* or *CIE-Lab*, the proposed one has the advantage of being a linear transform from the *RGB* color space, much like the *XYZ* or *YIQ*. However, its adaptiveness has the drawback of needing an estimate of the transform matrix for each image, which is sometimes computationally expensive for larger images due to the common iterative nature of the independent component analysis implementations. Then, an image subsampling method is also proposed to enhance the novel color space transform speed, efficiency and robustness. The new color space is used for a large set of test color images, and it is compared to traditional color space transforms, where we can clearly visualize its vast potential as a promising tool for segmentation purposes for example.

Keywords: Color Image Processing, Color Space Transform, Independent Component Analysis

1. INTRODUCTION

Computer vision is mainly about retrieving useful information from images, generally simulating the way the Human Vision System (HVS) performs it. In this way, color images are the natural information source and they are normally captured in the trichromatic *RGB* color space. Although widely used due to its simplicity, the *RGB* color space suffers from a high degree of correlation between its color channels, making harder the information extraction process from them. Therefore, many different color spaces have been suggested[1,2] and they are often used for achieving better results in several computer vision tasks such as color quantization, segmentation, compression, noise reduction, contrast enhancement, etc...[3–8]

Color space transforms are commonly based on fixed linear or non-linear operations from the *RGB* color space, with their respective advantages and drawbacks regarding for example the proportionality between the coordinates distance and the color difference, similarity to the HVS perception, separation of chromatic and achromatic channels, etc.... Nevertheless, none of the generic color spaces available such as *HSV*, *HSI*, *YUV*, *YIQ*, *CIE-Lab* or *CIE-Luv*, can really adapt to the color image content, performing in different ways for different computer vision tasks, so none of them is a real optimum for any kind of color images, having to choose by try and error which color space best fits to every specific application.[9–12] For this reason, the seek for new color space transforms is a constant concern in the color image processing research community. For example, and based on the color opponent model of the HVS, new color spaces have been defined in order to match the needs of color image segmentation[13] and quantization[14] algorithms.

However, in the specific case of adaptive color spaces, special attention is given to the $X_1X_2X_3$ color space based on the discrete *Karhunen-Loeve* (*K-L*) Transform,[2] which is commonly achieved by applying Principal Component Analysis (PCA) to the *RGB* color space data. It has the main advantage of being a linear transformation that leads to three new orthogonal channels that are uncorrelated to each other. This color space is widely accepted for image compression applications[10] and it has been extended to other applications such as Local Contrast Enhancement[15] and Face Recognition.[16]

Further author information: E-mail: esteban.vera@udec.cl, Address: Casilla 160-C, Concepcion, Chile.

Image Processing: Algorithms and Systems V, edited by Jaakko T. Astola, Karen O. Egiazarian, Edward R. Dougherty
Proc. of SPIE-IS&T Electronic Imaging, SPIE Vol. 6497, 64970P, © 2007 SPIE-IS&T · 0277-786X/07/$18

Nonetheless, in the early 80's, and after applying $X_1X_2X_3$ color space to a large amount of data for segmentation purposes, Ohta el al.[9] found an approximation to the *K-L* Transform by a fixed transform matrix, leading to the Ohta's color space $I_1I_2I_3$, which usually allows very similar results at much less computational cost, in despite of the loose of adaptiveness. Lately, a similar approximation has been performed after applying the *K-L* transform to the CIE-Lab space as well.[17]

Thinking in the constraints of the *K-L* color space, and also based on the successful applications to multispectral imagery,[18,19] in this paper we propose a novel color space transform based on the direct use of independent component analysis[20,21] (ICA) to entire *RGB* color space images. Lately, ICA has already being used in color image processing for many applications, but it has being used with small patches of color images to find basis functions that are finally useful for feature extraction and denoising.[22,23] However, in this particular new adaptive color space case, ICA finds a linear, but not necessarily orthogonal coordinate system where the *RGB* data is projected onto three new variables that are as statistically independent as possible from each other. Therefore ICA is a generalization of PCA and, like PCA, it has proven to be a useful tool for finding structure in data, so there are no reasons why not applying ICA to an entire color image and don't expect that at least the obtained results might equal or outperform the ones obtained by the *K-L* color space. Nonetheless, ICA has the disadvantage of being obtained by an iterative algorithm.

We test the proposed color space transform by applying it to different kind of images, and then comparing its results to the ones obtained by commonly used color spaces such as the *HSI*, *CIE-Lab*, $I1_I2_I3$ and $X_1X_2X_3$. From the results, we describe some special properties of the new color space, and we also show some potential applications.

This paper is organized as follows. In Section 2, a brief description of independent component analysis is presented. In Section 3 the new color space is described. A comparison between the proposed color space and classical ones applied to color images is shown in Section 4 . The conclusions of the paper are finally summarized in Section 5.

2. INDEPENDENT COMPONENT ANALYSIS

In this section an overview of independent component analysis[20,21] is presented. First the basics of the ICA model is described. Then, the fundamental principles of statistical independence are reinforced and characterized by higher order statistics. In this way several methods for achieving ICA are mentioned, and finally the used implementation is explained.

2.1. Definition of ICA

Assume that we observe n linear mixtures $x_1, \ldots, x_n$ of n independent components

$$x_j = a_{j1}s_1 + a_{j2}s_2 + \ldots + a_{jn}s_n, \forall j \tag{1}$$

where each mixture x_j and each independent component s_i is a zero-mean random variable. In vector notation the above mixing model is written as

$$\mathbf{x} = \mathbf{A}\mathbf{s} \tag{2}$$

where $\mathbf{A}$ is the mixing matrix whose elements are the coefficients a_{ij}. This statistical model is called independent component analysis, or ICA model. The ICA model is a generative model that describes how the observed data are generated by a process of mixing the components s_i, that cannot be directly observed otherwise. The mixing matrix is also assumed to be unknown, so all we observe is the random vector $\mathbf{x}$, and we must estimate both $\mathbf{A}$ and $\mathbf{s}$ from it.

The starting point for ICA is that the components s_i are statistically independent, which finally implies that the independent components must have nongaussian distributions. If we assume a square mixing matrix, so we have same number of observations than independent components, then after estimating the matrix $\mathbf{A}$ we can compute its inverse $\mathbf{W}$, and thus obtain the independent components by:

$$\mathbf{s} = \mathbf{W}\mathbf{x} \tag{3}$$

2.2. Statistical Independence

Considering two scalar-valued random variables y_1 and y_2, then this variables are independent if the information on the value of y_1 does not give any information on the value of y_2, and vice versa. In statistical terms, independence can be defined by probabilities densities. Let us denote by $p(y_1, y_2)$ the joint probability density function (pdf) of y_1 and y_2, and denote by $p_1(y_1)$ and $p_2(y_2)$ the marginal pdf of y_1 and y_2 respectively:

$$\begin{array}{l} p_1(y_1) = \int p(y_1, y_2) dy_2 \\ p_2(y_2) = \int p(y_1, y_2) dy_1 \end{array} \tag{4}$$

Then, y_1 and y_2 are independent if and only if its joint pdf is factorizable as

$$p(y_1, y_2) = p_1(y_1) p_2(y_2) \tag{5}$$

From the definition of independence above it can be derived the most important property of independent random variables. Given two functions h_1 and h_2, we always have

$$E\{h_1(y_1) h_2(y_2)\} = E\{h_1(y_1)\} E\{h_2(y_2)\} \tag{6}$$

If we know that two random variables are uncorrelated if their covariance is zero, then

$$E\{y_1 y_2\} - E\{y_1\} E\{y_2\} = 0 \tag{7}$$

Therefore, if the variables are independent, they are uncorrelated. On the other hand, uncorrelatedness does not imply independence.

2.3. ICA Implementation

The key for estimating the ICA model is nongaussianity. Following the Central Limit Theorem, a sum of independent random variables tends toward a gaussian distribution. Thus, a sum of two independent random variables has a distribution that is closer to gaussian than any of the two original random variables. If we assume that the data vector $\mathbf{x}$ is a mix of independent components, then the distribution of each mixed vector is more gaussian than any of the independent components in $\mathbf{s}$. Therefore if we can choose the unmixing matrix $\mathbf{W}$ in order to maximize the nongaussianity of each estimated component, then they will finally correspond to the independent components.

Thus, a measure of nongaussianity is needed in order to estimate the ICA model. Using a statistical approach, kurtosis will define if a distribution is subgaussian or supergaussian, and therefore is a good measure of the nongaussianity degree. On the other hand, by using an information theory approach, negentropy is an adequate choice.

Other approaches to solve the ICA model are related to minimization of mutual information, maximum likelihood by infomax, and projection pursuit, but they are very related to the maximization of nongaussianity at the end.

In this case we will make use of the widely used and accepted ICA algorithm called FastICA.[24] The preprocessing steps to apply the ICA method is basically: centering the data, or removing its mean value leading to zero-mean variables; and whitening the data, leading to uncorrelated unit variance data. Centering is a very trivial step, and whitening can be easily achieved by Principal Component Analysis, or PCA. The algorithm is of an iterative nature, and basically it needs to setup initially the startup for the unmixing matrix $\mathbf{W}$ and the selection of the nonlinear function used to estimate an approximation value for the negentropy.

3. NEW COLOR SPACE TRANSFORM

The adaptive color space transform here proposed is based on the application of independent component analysis to a *RGB* color image. At the end this is an improved, and generalized natural extension of the $X_1X_2X_3$ *Karhunen-Loeve* color space obtained by using PCA.[2]

3.1. Description

In this particular color space transform case, each *RGB* channel is treated as a sample measurement with a different point-of-view of the same scene, which can lead us to discover up to three different independent components that are supposed to be mixed in each observation in the R, G and B channels. The only big assumption is that the statistical distributions of the unknown independent components are nongaussian, then what the ICA algorithm pursues is to find the best tridimensional linear projection into the *RGB* cube that maximize the nongaussianity of each estimated component, that can be at the end statistically independent from each other.

We are assuming that each of the three *RGB* channels has a mix of three independent (nongaussian) components, which might not be necessarily true, so what we are finally doing at the end is seeking for three components the most independent as possible. Every resulting estimated independent component is expected to be more uncorrelated to each other compared to the original *RGB* channels, and also to other color spaces. Of course, each of these three supposed independent components can contain a mix of even more real independent components, because we will commonly have more independent components than mixtures, but we are finally constrained to estimate a maximum of three.

3.2. Practical Considerations

To apply the proposed transform first we reorder each *RGB* channel of a given image into a vector, and then once we apply the independent component analysis algorithm (FastICA[24]) to the three vectors we get as a result the separation (unmixing) matrix $\mathbf{W}$, which will define our color space transform matrix for a particular image, like any linear color space transform. This separation matrix, and its inverse (the mixing matrix $\mathbf{A}$), can be further used to perform the color space transform back and forth for the same image. Then, some clear advantages of the adaptive color space proposed here are: the linearity of the transform and, of course, its adaptiveness. In addition, we should state as a major advantage the lack of constraints regarding the orthogonality of the projections, such as in PCA, which is an extra degree of freedom to perform an estimation that fits better the data distribution in the statistical independence sense. However this extra degree of freedom is also adding complexity to the ICA algorithm itself, which sometimes leads that the tuning of the FastICA algorithm can become tricky. However, the worst result we could get is as good or bad as performing only the whitening on the data, obtaining the same result as the *K-L* only transformation.

Typically we choose as a starting mixing matrix for the iteration algorithm the identity matrix, but a random vector could also be used. The main difference is that if we apply the algorithm several times to the same image, the order of the estimated independent components can change randomly as well, but generally the same results are achieved. The other important point is the selection of the nonlinearity for the algorithm. We typically selected the tanh, but normally any other choice used to work well in the same way. The only problem was related when no convergence was achieved, so the change of nonlinearity sometimes helped in making it work.

Additionally, for larger images the convergence time in a normal Personal Computer (PC) can be too long for certain difficult images in particular, so a subsampling scheme helped to accelerate the convergence time, and also helped in making the estimation more robust. At the beginning we tried fractal subsampling scanning as proposed in,[25] but at the end using normal vector downsampling was enough to guarantee proper and repeatable results. In all the test images used, we tried with good confidence up to a factor of 100 in downsampling leading to similar results, but with a significative reduction on the number of iterations needed, increasing even further the speed up of the convergence time. It seems that there are less distraction points that used to confuse the algorithm, avoiding local minima for example.

Finally, it is worth to mention that the FastICA algorithm includes the mean removal for the initial data vectors and also realizes the whitening to the data through PCA, so the preprocessing step is the entire *K-L* $X_1X_2X_3$ color space transform.

4. RESULTS

In order to test the behavior of the new adaptive color space transform, we applied it to a large collection of color images extracted from the Berkeley Segmentation Database,[26] the Image Quality Assessment Database,[27] and

the USC-SIPI Image Database[28] where we extracted some classical color test image processing such as Lenna, Peppers and Mandrill.

The obtained new color space projections are identified by $IC_1IC_2IC_3$, and we typically compared them to the original *RGB* channels and also to the ones obtained by applying the: *HSI*, *CIE-Lab*, $I_1I_2I_3$ (Ohta), and $X_1X_2X_3$ *K-L* color space transforms. However due to space limitations, only one sample picture of each image database was selected to be used as the test images used throughout this paper, as shown in figure 1.

(a) (b) (c)

Figure 1. Color Test Images. a) Mandrill. b) Monarch. c) Face.

4.1. Overall Color Space Comparison

We will start the analysis by checking the results obtained for the Mandrill image[28] in figure 2. This image is very special and is a tough test for any image processing algorithm, including a color space. In fact, it took several iteration for the FastICA algorithm to converge, so after using downsampling it was fine, but still difficult compared to most of the images.

First of all, it is easy to realize that the *RGB* color space is highly correlated, specially between the G and B channels that appear like different black and white versions of the original image. Nonetheless, due to the prominent big red nose, the R channel looks particularly different than the usual. In the corresponding left columns, we tried to align the channels related to the luminance estimation component of each color space, and we can see that all of them are quite similar, regardless some brighter or darker appearance. However, special attention is given to the IC_1, where compared to its counterparts the eyes look with less bright than the expected, and therefore it might not be a good luminance estimation as the *K-L* case.

Looking at the second column, it can be seen that the nose is noticeable in all the shown channels, except in the *HSV* channel H where the image should be inverted to see this effect. Both I_2 and X_2 channels emphasize not only the nose but also the eyes and the yellow beard of the ape. On the other hand, channel IC_2 looks more like channel a in *Lab*, where the nose is evidently separated from the rest, and even the eyes are less brighter.

After watching the third columns, it can be seen that *HSV* S and *Lab* b channels are quite similar, still clearly showing the nose and the eyes, which is comparable to channels X_2 and I_2 as well, in despite of a slightly darker nose. In addition, IC_3 and X_3 are very alike, showing the ape yellowish hair, beard and the eyes, which is even stronger in the ICA color space. Therefore, it seems that the proposed color space found projections much like in the direction of the real color of the nose, the eyes, and in a sort of color average.

Following the next example, we will check the results for the Monarch image[27] in figure 3, which is a butterfly picture where the yellow and pink colors dominates the scene.

In the same way as the previous analysis we started by examining the *RGB* channels, where a strong correlation is seen between channels R and G, and channel B is mostly showing the white part of the flower plants and the white butterfly points as well. Analogous to , all luminance estimates are in the left column, where it can be seen that most of them (I, I_1 and X_1) are very similar to the G channel, and the L in *Lab* is very similar to the R channel. On the other hand, the IC_1 channel is resembling the B channel in some way, reinforcing the white parts of the image, and hardly representing a luminance estimate for the original color image.

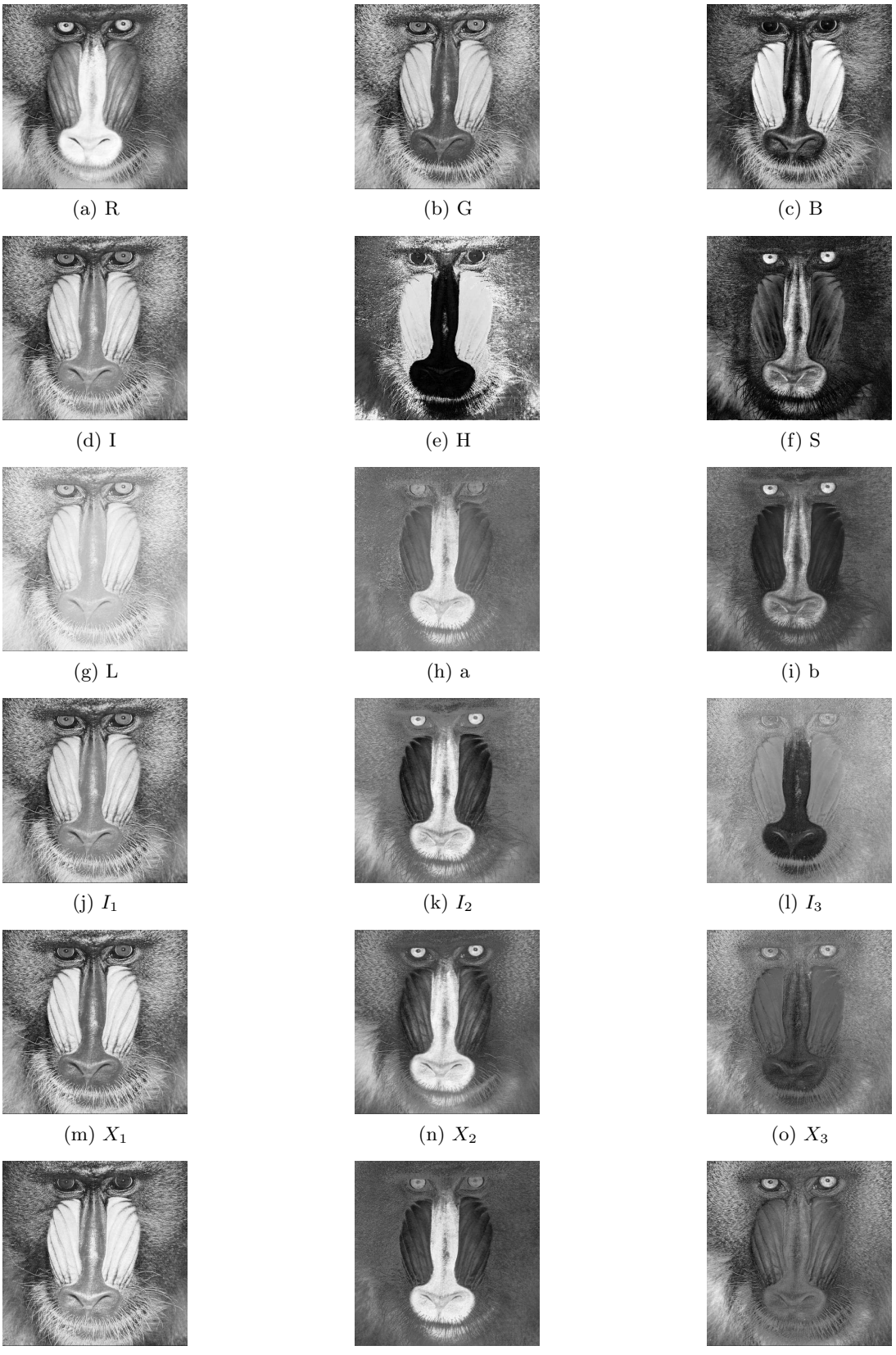

(a) R (b) G (c) B

(d) I (e) H (f) S

(g) L (h) a (i) b

(j) I_1 (k) I_2 (l) I_3

(m) X_1 (n) X_2 (o) X_3

(p) IC_1 (q) IC_2 (r) IC_3

Figure 2. Mandrill represented in several Color Spaces: a-c)RGB; d-f)HSI; g-i)Lab; j-l)Ohta; m-o)PCA; p-r)ICA.

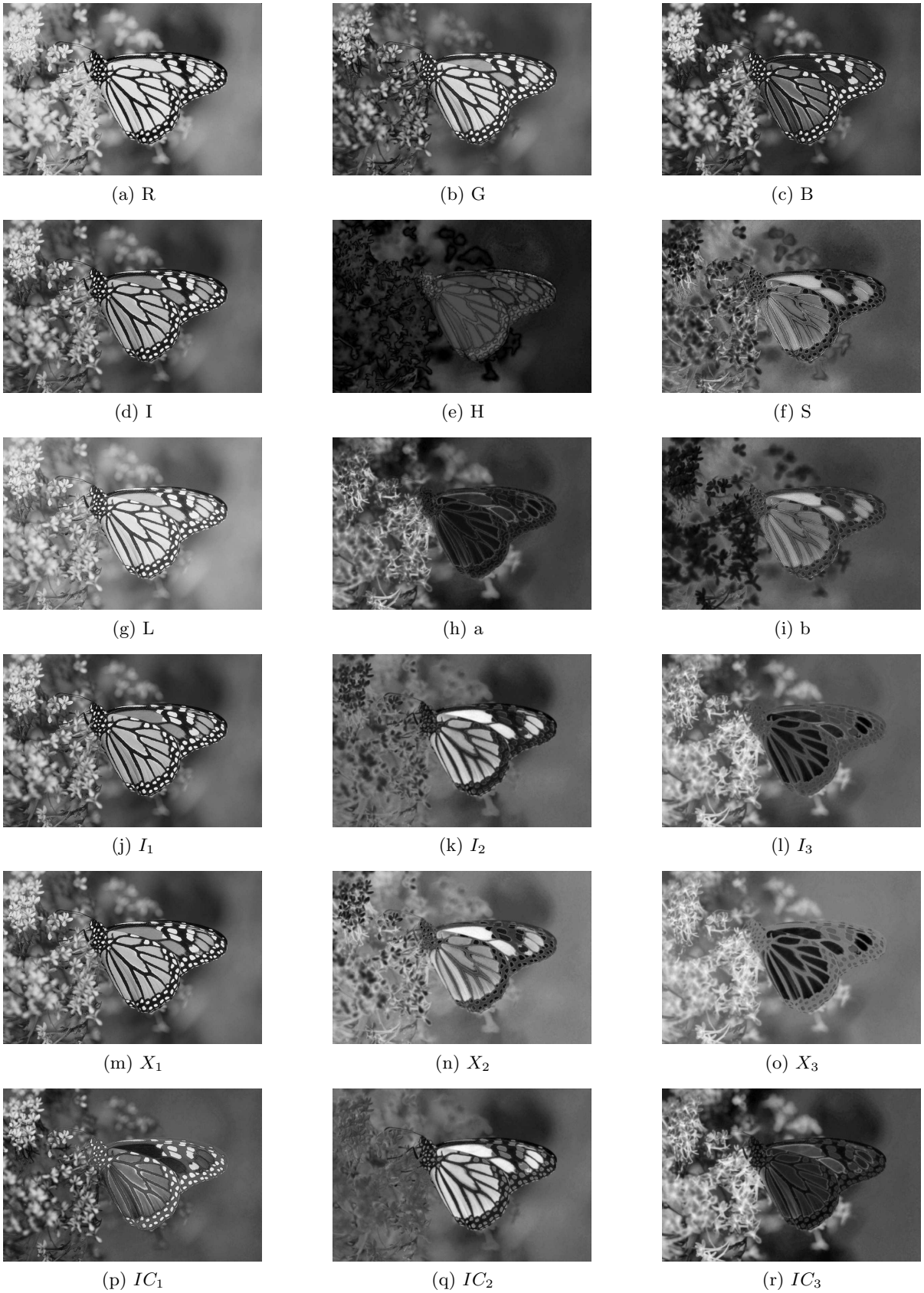

(a) R (b) G (c) B

(d) I (e) H (f) S

(g) L (h) a (i) b

(j) I_1 (k) I_2 (l) I_3

(m) X_1 (n) X_2 (o) X_3

(p) IC_1 (q) IC_2 (r) IC_3

Figure 3. Monarch represented in several Color Spaces: a-c)RGB; d-f)HSI; g-i)Lab; j-l)Ohta; m-o)PCA; p-r)ICA.

Checking the remaining channels, it can be seen that the *HSI S* channel is very similar to the b channel in *Lab*, representing mostly the butterfly wings, analogous to the behavior of channels I_2, X_2 and IC_2, where mainly only the yellow part of the wings is stand out. Although, X_2 is displaying parts of the pink flower plants, which is even more noticeable in channels I_3 and X_3. However, parts of the butterfly wings are still visible, but they almost disappear in channels a from *Lab*, and the proposed IC_3, where only the pink flower is clearly present.

From both analyzed images, it can be seen that instead of generating one achromatic channel plus two chromatic ones, the proposed adaptive color space generates projections in the chromatic direction of what we could call the main independent colors. In this way, at least some of the projections are very similar to the ones achieved by the widely spread used *CIE-Lab* color space, but through a linear transformation.

In addition, we can notice some huge separation of certain noticeable and specific image features projected onto the different transformed independent channels, just like our own HVS performs, which might enhance later segmentation and recognition tasks for example, compared mainly to the results obtained by the *K-L* transform.

Similar behavior is mainly found in most of the images used but not shown here, However, this is not the case for all the images, because some of them never converged at all, maybe because they do not accomplish the requirement for the existence of independent components, such as the desired nongaussianity.

4.2. Adaptive Color Space Comparison

Then, a comparison on the performance of both adaptive color space transform described here is presented. In this sense, we would like to project back to the original *RGB* color space every channel by itself, filling the other channels with zeros. Therefore, we will be able to see the colors where each channel are mainly projected. Anyway, some considerations may be taken in account. For example, for almost all of the X_2 and X_3 projected components derived from the *K-L* transform, a gain was applied in order to proper visualize the data. Furthermore, some projections in both cases have negative values, so when they are projected back onto the *RGB* plane they cannot be visualized directly, so sometimes we have some truncation on the visualizations, which allow us to see some behavior in the case of hard thresholding as a segmentation approach. Finally, in any case, by summing all the projections at the *RGB* level we get the reconstruction of the original color image.

First, the results for the Mandrill image are shown in figure 4. In the case of the *K-L* transform results, it can be seen that the first component is projected onto a light blue color. On the other hand the other two components are projected into red and green colors respectively. For the ICA results it is clear that the projections are in a blue-violet, red, and yellow colors, most likely the real images main colors at a first sight. In addition, the nose is almost left alone in IC_2, and the eyes and hair are isolated in IC_3.

Then, by checking the Monarch image in figure 5, we can see a similar behavior than the previous analysis. For the first *K-L* component we have a sepia like projection, which is clearly the luminance component, and the second and third components are again projected onto green and red colors. Now seeing the ICA components, the first one is obviously not a valid luminance estimation, and it displaying all the related white features of the original image. In the same way, the yellow part of the butterfly wing is clearly separated from the rest of the scene in IC_2, and in the same yellow color, and also the pink flowers are isolated in component IC_3 in the same color as in the original image.

Last, in figure 6 we present the color projections of the last image, Face,[26] whose channel values for the other color spaces were not shown here like for the other presented images due to space limitations.

For the Face image then, similar characteristics can be seen for the *K-L* projections, where the first component resides again in a sepia like color, and the X_2 component clear separates the skin projected onto a red color, while X_3 displays mainly the lips in a violet like one. In the case of the ICA projection, the components are very analogous to the *K-L* ones, however as discussed before, the first component is not necessarily a luminance estimation, showing signs of representing the white color in the original image. So in the case of IC_2, the skin is separated in the same way as in X_2, however the color is more accurate regarding the skin. And in the last component, the lips appear in a more realistic red color.

In conclusion we can say that what was found by Ohta[9] is right. The first component X_1 is always a sort of summed average of all *RGB* channels, and X_2 and X_3 are projections of the form $(R - B)$ and $(G - R - B)$, which coincides with the fact of finding positive projections in the red and green colors mostly. In addition, all

(a) X_1 (b) X_2 (c) X_3

(d) IC_1 (e) IC_2 (f) IC_3

Figure 4. Manrill Image. a-c)PCA Color Projections; d-f)ICA Color Projections.

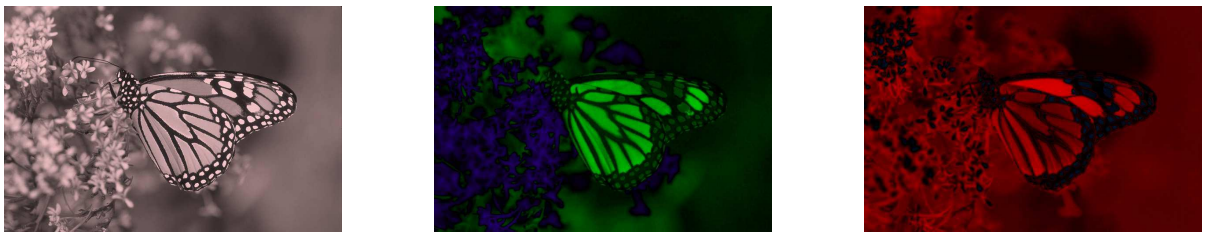

(a) X_1 (b) X_2 (c) X_3

(d) IC_1 (e) IC_2 (f) IC_3

Figure 5. Monarch Image. a-c)PCA Color Projections; d-f)ICA Color Projections.

projections from both adaptive color spaces in gray level at least seems to be quite similar, trying to separate and enhance image features. Nonetheless, from the color projections it can be seen that the ICA projections shows image features that are even more enhanced and separated, and also the projected colors are more realistic compared to the original color images. This can be related to the fact of the orthogonality constraint in the PCA projections, which may allow to match one of the image colors, but not more than that.

Finally to end our tests on color images, we would like to present the following experiment, where we play with the latest Face image by manipulating the independent components $IC_1IC_2IC_3$. In this case we apply gain factors to IC_2 (the skin) and IC_3 (the lips). In figure 7 some examples of mixed gain factors applied to the mentioned components are displayed. There, it is hard to notice which one is the original image (in the middle), because all of them look quite natural. So in this particular case we can say that we found three main components of the color image that are not only uncorrelated, but also independent, and thus nongaussian. Then we could also call them the independent colors of the image.

(a) X_1 (b) X_2 (c) X_3

(d) IC_1 (e) IC_2 (f) IC_3

Figure 6. Face Image. a-c)PCA Color Projections; d-f)ICA Color Projections.

(a) IC_1 (b) IC_2 (c) IC_3 (c) IC_3 (c) IC_3

Figure 7. Face Image Experiment. a)$1.75 \times IC_2 + 0.7 \times IC_3$. b)$1.35 \times IC_2 + 1.8 \times IC_3$; c)Original Image; d)$0.3 \times IC_2 + 1.3 \times IC_3$; e)$0.5 \times IC_2 + 0.7 \times IC_3$.

5. CONCLUSIONS

We presented a new color space transform. It is an image dependent adaptive transform based on the application of independent component analysis to the *RGB* data. Furthermore it is a linear and reversible color space transform that provides three new not necessarily orthogonal coordinate axes where the projected data is as much as statistically independent as possible, and therefore highly uncorrelated. When compared to common fixed color space transforms it shows in the chosen test images impressive results, separating color features in a very special way. Nevertheless, the new color representation lacks of a luminance channel, but on the other hand it utilizes its third channel to display additional color features. Also, when compared to other adaptive color spaces such as the *Karhunen-Loeve* one, it seems to outperform it because it is able to spread the information

over the different channels, separating color features in a unseen way, instead of concentrating the energy in the first component like in the *K-L* case, which can be a great advantage in segmentation of color images. As seen in the *RGB* color projections, the proposed color space can adapts in a better way to fit the data distribution in any color direction, with no orthogonality constraints, allowing interesting image processing manipulations. However, it is not usable for all kind of color images, because the statistical constraints regarding performing independent component analysis successfully are not always accomplished by the data itself. It was also shown that by using downsampling in the input data, alleviates the ICA algorithm work, making it faster and even more robust. Therefore, the application of independent component analysis as a new color space transform tool is more than advisable, in despite of the algorithm convergence issue. So it is finally up to the image processing research community to adopt the proposed color space in order to test it extensively and finally proof it as an useful alternative to novel or even older computer vision algorithms.

Acknowledgments

The authors thank the Chilean Council for Science and Technology, CONICYT, through its project ALMA-CONICYT 30105006 and a doctorate studies scholarship, and also thank the Department of Electrical Engineering of the University of Concepcion for their financial support.

REFERENCES

1. G. Sharma and J. Trussell, "Digital color imaging," *IEEE Transactions on Image Processing* **6**, pp. 901–931, July 1997.
2. W. K. Pratt, *Digital Image Processing*, John Wiley & Sons, 3rd ed., 2001.
3. T. Uchiyama and M. A. Arbib, "Color image segmentation using competitive learning," *IEEE Transactions on Pattern Analysis and Machine Intelligence* **16**, pp. 1197–1206, December 1994.
4. T.-H. Yu, "Color image enhancement in a new color space," *Proceedings of SPIE* **2727**, pp. 1462–1472, 1996.
5. M. Mirmehdi and M. Petrou, "Segmentation of color textures," *IEEE Transactions on Pattern Analysis and Machine Intelligence* **22**, pp. 142–159, February 2000.
6. Y. Deng, B. S. Manjunath, C. Kenney, M. S. Moore, and H. Shin, "An efficient color representation for image retrieval," *IEEE Transactions on Image Processing* **10**, pp. 140–147, January 2001.
7. L. Lucchese and S. K. Mitra, "Colour segmentation based on separate anisotropic diffusion of chromatic and achromatic channels," *IEE Proceedings in Vision, Image, and Signal Processing* **148**, pp. 141–150, June 2001.
8. I. Vanhamel, I. Pratikakis, and H. Salem, "Multiscale gradient watersheds of color images," *IEEE Transactions on Image Processing* **12**, pp. 617–626, June 2003.
9. Y. Ohta, T. Kanade, and T. Sakai, "Color information for region segmentation," *Computer Graphics and Image Processing* **13**, pp. 222 – 241, July 1980.
10. S. Han, B. Tao, T. Cooper, and I. Tastl, "Comparison between different color transformations for jpeg 2000," *Proceedings of the IS&T PICS* , pp. 259–263, March 2000.
11. L. Lucchese and S. K. Mitra, "Color image segmentation: A state-of-the-art survey," *Proc. Indian National Science Academy (INSA-A)* **67**, pp. 301–221, March 2001.
12. P. Guo and M. R. Lyu, "A study on color space selection for determining image segmentation region number," *Proceedings of the International Conference on Artificial Intelligence* , pp. 1127–1132, June 2000.
13. T. Gevers, "Image segmentation and similarity of color-texture objects," *IEEE Transactions on Multimedia* **4**, pp. 509–516, December 2002.
14. J.-P. Braquelaire and L. Brun, "Comparison and optimization of methods of color image quantization," *IEEE Transactions on Image Processing* **6**, pp. 1048–1052, July 1997.
15. L. Meylan and S. Susstrunk, "High dynamic range image rendering with a retinex-based adaptive filter," *IEEE Transactions on Image Processing* **15**, pp. 2820–2830, September 2006.
16. C. F. J. III and A. L. Abbott, "Optimization of color conversion for face recognition," *Eurasip Journal on Applied Signal Processing* (4), pp. 522–529, 2004.

17. Y. Chen, P. Hao, and A. Dang, "Optimal transform in perceptually uniform color space and its application in image coding," *Lecture Notes in Computer Science* **3211**, pp. 269–276, 2004.
18. S. Rajagopalan and R. A. Robb, "Independent component analysis assisted unsupervised multispectral classification," *Proceedings of the SPIE* **5029**(1), pp. 725–733, SPIE, 2003.
19. Q. Du, I. Kopriva, and H. Szu, "Independent-component analysis for hyperspectral remote sensing imagery classification," *Optical Engineering* **45**(1), p. 017008, 2006.
20. A. Hyvarinen, J. Karhunen, and E. Oja, *Independent Component Analysis*, John Wiley & Sons, 2001.
21. J. V. Stone, *Independent Component Analysis: A Tutorial Introduction*, MIT press, 2004.
22. P. Hoyer and A. Hyvrinen, "Independent component analysis applied to feature extraction from colour and stereo images," *Network: Computation in Neural Systems* **11**, pp. 191–210, August 2000.
23. T.-W. Lee and M. S. Lewicki, "Unsupervised image classification, segmentation and enhancement using ica mixture models," *IEEE Transactions on Image Processing* **11**, pp. 270–279, March 2002.
24. A. Hyvrinen, "Fast and robust fixed-point algorithms for independent component analysis," *IEEE Transactions on Neural Networks* **10**, pp. 626–634, May 1999.
25. N. Papamarkos, A. E. Atsalakis, and C. P. Strouthopoulos, "Adaptive color reduction," *IEEE Transactions on Systems, Man, and Cybernetics-Part B: Cybernetics* **32**, pp. 44–56, February 2002.
26. D. Martin, C. Fowlkes, D. Tal, and J. Malik, "A database of human segmented natural images and its application to evaluating segmentation algorithms and measuring ecological statistics," in *Proc. 8th Int'l Conf. Computer Vision*, **2**, pp. 416–423, July 2001.
27. H. R. Sheikh, Z. Wang, L. Cormack, and A. C. Bovik, "Live image quality assessment database," *http://live.ece.utexas.edu/research/quality* .
28. A. G. Weber, "The usc-sipi image database," *http://sipi.usc.edu/database/* .